Comparative Analysis of Classifiers for Higher-order Statistics-based Modulation Recognition in Cooperative STBC-OFDM

Brahim Dehri[1], Hakima Moulay[2], Ahmed Amine Daikh[1,3], and Mokhtar Besseghier[3]

[1]*University Centre of Naama, Naama, Algeria,*
[2]*University of Sidi Bel Abbes, Sidi Bel Abbes, Algeria,*
[3]*University of Mustapha Stambouli, Mascara, Algeria*

https://doi.org/10.26636/jtit.2026.1.2299

Abstract — Precise classification of modulation in cooperative relaying networks remains challenging in the presence of carrier frequency offset (CFO) and imperfect channel state information (CSI). This paper conducts a comprehensive comparative analysis of automatic modulation classification (AMC) methods for distributed space-time block-coded orthogonal frequency division multiplexing (DSTBC-OFDM) systems under these impairments. A unified simulation framework is developed that combines pilot-assisted CFO and CSI estimation with higher-order statistics (HOS)-based feature extraction. Four widely used machine learning classifiers, i.e. feedforward neural network, support vector machine, random forest classifier, and adaptive boosting, are benchmarked under identical channel and noise conditions. Monte Carlo simulations are performed across varying SNR levels and fading scenarios, enabling a fair assessment of classification accuracy, robustness to residual estimation errors, and relative computational complexity. The results provide practical insights into the strengths and limitations of each classifier in cooperative STBC-OFDM environments, offering valuable guidelines for selecting AMC techniques in future cooperative wireless systems.

Keywords — automatic modulation classification, CFO estimation, CSI, DSTBC-OFDM, higher-order statistics, machine learning

1. Introduction

The design of blind receivers for cooperative relaying (CR) networks remains a challenge due to the combined effects of carrier frequency offset (CFO) and imperfect channel state information (CSI). In distributed space-time block-coded orthogonal frequency division multiplexing (DSTBC-OFDM) systems, these impairments complicate frequency synchronization, channel estimation, and modulation recognition, especially in cooperative scenarios where multiple relay nodes introduce additional CFOs and diverse channel conditions.

Cooperative communications exploit the diversity by employing intermediate relay nodes to form virtual multiple-input multiple-output (MIMO) channels between a source and a destination [1]. In a typical half-duplex relaying set-up, transmission occurs in two phases: the source broadcasts to both destination and relay in the first phase, and in the second phase, the relay forwards the received signal to the destination [2]. Among the various relaying strategies, the amplify-and-forward (AF) technique remains attractive due to its low complexity, while the decode-and-forward (DF) method can provide improved reliability at the expense of higher processing demands [3], [4]. DSTBC is often applied in AF systems to preserve spectral efficiency and improve diversity gains.

Orthogonal frequency division multiplexing (OFDM) is widely adopted for wireless broadband communications due to its robustness against frequency-selective fading and its ability to simplify the equalization process [5]. The combination of DSTBC and OFDM creates a flexible and high-performance framework for cooperative wireless systems, capable of mitigating multipath fading while leveraging spatial diversity. However, achieving these benefits in practice requires an accurate estimation of the CFO and CSI [6], as errors in either parameter directly affect data detection and, consequently, precise classification of the modulation.

Automatic modulation classification (AMC) plays a central role in both civilian and military applications, enabling spectrum monitoring, interference detection, adaptive waveform selection, and electronic warfare countermeasures [7]. AMC techniques are generally classified into maximum likelihood (ML) and feature-based (FB) approaches [8]. Although ML methods can be optimal, they are computationally expensive and require detailed signal models, making FB approaches – especially those relying on higher-order statistics (HOS) – attractive due to their good balance between complexity and robustness [9].

In FB-based AMC, the classifier is as important as the feature set. Popular single-learner models include support vector machines (SVM) and neural networks, while ensemble learning methods such as random forest classifier (RFC) and adaptive boosting (AdaBoost) have shown promise in improving classification performance [10]. However, most AMC studies focus on non-cooperative transmission scenarios, and only limited work has examined cooperative DSTBC-OFDM systems, where CFO estimation, CSI acquisition, and classification must be performed jointly under more challenging conditions [11], [12].

Furthermore, existing cooperative AMC research rarely benchmarks multiple classifier types within the same feature extraction and channel-impairment framework, leaving practitioners with little guidance on optimal classifier selection for this context.

To bridge these gaps, this work introduces an integrated framework that unifies realistic channel estimation, synchronization, and intelligent classification in cooperative DSTBC-OFDM networks. Unlike previous studies that treated estimation and classification separately or relied on idealized assumptions, this approach combines pilot-assisted CFO and CSI estimation with higher-order statistical features to enable blind and robust modulation recognition.

The novelty lies in the systematic benchmarking of single and ensemble classifiers under identical channel and feature conditions. This contribution is not extensively addressed in the prior literature.

This paper fills this gap by conducting a comprehensive benchmarking study of single- and ensemble-learning classifiers for HOS-based AMC in cooperative DSTBC-OFDM systems using AF relaying. A unified simulation framework is developed that integrates pilot-assisted CFO estimation via virtual subcarriers (VSCs), pilot-based CSI estimation, and HOS feature extraction, followed by classification with feedforward neural networks (FFNN), SVM, RFC, and AdaBoost. The evaluation compares classification accuracy, robustness to residual estimation errors, and computational complexity under varying SNR and fading conditions.

Table 1 shows the abbreviations and notations used in this article.

Tab. 1. Used notation.

Upper case bold letters	Matrices
Lower case bold-italic letters	Column vectors
$(\cdot)^*$	Complex conjugate
$(\cdot)^T$	Transpose operator
$(\cdot)^\sharp$	Pseudo-inverse
$(\cdot)^H$	Hermitian transpose
$\otimes$	Kronecker products
$\Re[\cdot]$	Real parts
$\Im[\cdot]$	Imaginary parts
$E\{\cdot\}$	Expected value of a random variable
diag[**x**]	Diagonal matrix (**x** is main diagonal)
$\mathbf{D}_N(\mathbf{h}) = \text{diag}[\mathbf{h}]$	Diagonal matrix of size $N \times N$
$\lvert\cdot\rvert$	Modulus of a complex number
$\lVert\cdot\rVert$	Euclidean norm
$\text{tr}(\mathbf{X})$	Trace of the matrix $\mathbf{X}$
$[\mathbf{x}]_m$	m-th entry of the column vector $\mathbf{x}$
$[\mathbf{A}]_{k,m}$	(k,m)-th entry of a matrix $\mathbf{A}$
$\mathbf{I}_N$	Identity matrix of size $N \times N$
$[\mathbf{F}_N]_{m,n}$	FFT matrix of size $N \times N$
$\mathbb{F}_p$	FFT of pilot symbols
$\mathbb{F}_d$	FFT of data symbols

2. System Model

The concept behind the cooperative DSTBC-OFDM technique is to implement a communication process between source S and destination D nodes in a distributed way with the help of communicating nodes R that act as relays [1]. In this paper, we consider that only one antenna occupies the S and R terminals, while one or two receive antennas can be used at the D terminal (Fig. 1).

The source and relay nodes cooperate using the AF protocol based on the architecture of Alamouti STBC-OFDM for data and pilot blocs are given by:

$$\begin{cases} \mathbb{S}_i = \begin{bmatrix} \mathbf{S}_{2i} & \mathbf{S}_{2i+1} \\ -\mathbf{S}^*_{2i+1} & \mathbf{S}^*_{2i} \end{bmatrix} \\ \mathbb{P}_i = \begin{bmatrix} \mathbf{P}_{2i} & \mathbf{P}_{2i+1} \\ -\mathbf{P}^*_{2i+1} & \mathbf{P}^*_{2i} \end{bmatrix} \end{cases}, \tag{1}$$

$$\begin{cases} \mathbf{S}_{2i+m} = \text{diag}(\mathbf{s}_{2i+m}) \\ \mathbf{s}_{2i+m} = \left[s_{2i+m}(0), s_{2i+m}(1), \Phi, s_{2i+1}(N_d - 1) \right] \\ \mathbf{P}_{2i+m} = \text{diag}(\mathbf{p}_{2i+m}) \\ \mathbf{p}_{2i+m} = \left[p_{2i+m}(0), p_{2i+m}(1), \Phi, p_{2i+1}(N_d - 1) \right] \end{cases}, \tag{2}$$

where S_{2i+m} and P_{2i+m} are the $(2i+m)$-th data and pilot symbols, respectively, and $m \in \{0,1\}$ is the index of two successive data and pilot vectors for the i-th STBC coding matrix.

We consider an OFDM modulation with N subcarriers. Only N_e from N subcarriers are used, the remaining $N_{vsc} = N - N_e$ subcarriers represent the virtual subcarriers (VSCs) [13]. The active subcarriers N_e are divided into two subsets of N_p subcarriers for pilot symbols and N_d subcarriers for information symbols. We define $\mathbf{i}_\beta = \{\beta_1, \ldots, \beta_{N_p}\}$ as a subset of indexes for pilot tones and $\mathbf{i}_\alpha = \{\alpha_1, \ldots, \alpha_{N_d}\}$ as a subset of indexes of subcarriers carrying data symbols.

The insertion of the pilot sub-block $\mathbf{p}_{2i+m}$ into the information sub-block $\mathbf{s}_{2i+m}$ is realized by:

$$\mathbf{z}_{2i+m} = \mathbf{Q}^\beta_{N_e} \mathbf{p}_{2i+m} + \mathbf{Q}^\alpha_{N_e} \mathbf{s}_{2i+m}\,, \tag{3}$$

where:

$$\begin{cases} \mathbf{Q}^\alpha_{N_e} = \mathbf{I}_{N_e}\{\boldsymbol{\alpha}\} = \left[\mathbf{e}^{(\alpha_1)}_{N_e} \mathbf{e}^{(\alpha_2)}_{N_e} \ldots \mathbf{e}^{(\alpha_{N_d})}_{N_e} \right] \\ \mathbf{Q}^\beta_{N_e} = \mathbf{I}_{N_e}\{\boldsymbol{\beta}\} = \left[\mathbf{e}^{(\beta_1)}_{N_e} \mathbf{e}^{(\beta_2)}_{N_e} \ldots \mathbf{e}^{(\beta_{N_p})}_{N_e} \right] \end{cases}, \tag{4}$$

are the permutation matrices [5].

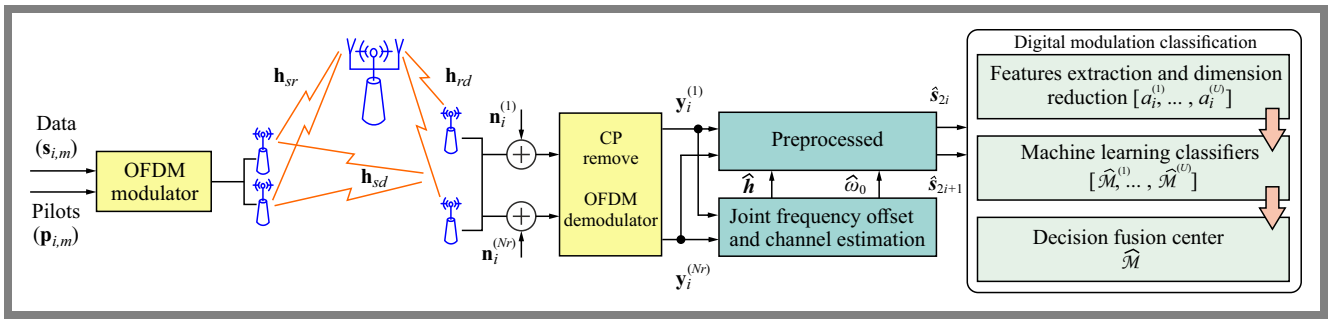

Fig. 1. Baseband equivalent model of the cooperative relaying DSTBC-OFDM system.

N_{vsc} virtual subcarriers are added to $\mathbf{z}_{2i+m}$ to form the vectors $\hat{z}_{2i+m}$. The multiplexed sub-blocks $\hat{\mathbf{z}}_{2i+m}$ are left multiplied by the inverse fast Fourier transform (IFFT) matrix $\mathbf{F}_N^H$ to form the vectors $\widetilde{\mathbf{z}}_{2i+m}$. Before emission, cyclic prefix (CP) of length N_{cp} must be inserted by multiplication with an appropriate matrix $\mathbf{T}_{cp} = [\mathbf{I}_{N_{cp}\times N}^T, \mathbf{I}_N^T]^T$. The i-th transmitted STBC matrix becomes:

$$\mathbf{x}_i = \begin{bmatrix} \mathbf{x}_{2i}\mathbf{x}_{2i+1} & \\ -\mathbf{x}_{2i+1}^* & \mathbf{x}_{2i}^* \end{bmatrix} = (\mathbf{I}_2 \otimes \mathbf{T}_{cp}) \begin{bmatrix} \tilde{\mathbf{z}}_{2i} & \tilde{\mathbf{z}}_{2i+1} \\ -\tilde{\mathbf{z}}_{2i+1}^* & \tilde{\mathbf{z}}_{2i}^* \end{bmatrix} . \quad (5)$$

The two sub-blocks $[x_{2i}, -\mathbf{x}_{2i+1}^*]$ correspond to symbols conveyed by the source in the time slots 1 and 2, whereas $[\mathbf{x}_{2i+1}, x_{2i}^*]$ refers to the one forwarded by the relay in the time slots 3 and 4.

2.1. DSTBC Design

During the first broadcasting phase, the two sub-blocks $[\mathbf{x}_{2i}, -\mathbf{x}_{2i+1}^*]$ are broadcast to R and D nodes with a transmitted power p_s.

At reception, we remove the cyclic prefix by multiplying each received STBC block by $\mathbf{R}_{cp}$ where $\mathbf{R}_{cp} = [\mathbf{0}_{N\times N_{cp}}, \mathbf{I}_N]$. In this paper, we adopt the model developed in [7] where the CFO between the source and the relay is not considered. As we assume that the CFO is the same for all receive antennas, that is true for the case where CFO is generated by the carrier frequency mismatch between the transmit and the receive oscillators. Next, the signals received by the n_r-th antenna of the destination node and by the unique antenna at the relay node are given by Eqs. (6) and (7).

$$\mathbb{y}_{i,sd}^{(n_r)} = \begin{bmatrix} \mathbf{y}_{i,sd}^{n_r}[1] \\ \mathbf{y}_{i,sd}^{n_r}[2] \end{bmatrix} = \sqrt{p_s}\,\mathbb{D}_N(\omega_0) \cdot \left(\mathbb{F}_p^H \begin{bmatrix} \mathbf{P}_{2i} \\ -\mathbf{P}_{2i+1}^* \end{bmatrix} \mathbf{\Gamma}_p + \mathbb{F}_d^H \begin{bmatrix} \mathbf{S}_{2i} \\ -\mathbf{S}_{2i+1}^* \end{bmatrix} \mathbf{\Gamma}_d \right) \mathbf{h}_{i,sd}^{(n_r)} + \boldsymbol{\eta}_{i,sd}^{(n_r)} \quad (6)$$

$$\mathbb{y}_{i,sr} = \begin{bmatrix} \mathbf{y}_{i,sr}[1] \\ \mathbf{y}_{i,sr}[2] \end{bmatrix} = \sqrt{p_s} \left(\mathbb{F}_p^H \begin{bmatrix} \mathbf{P}_{2i} \\ -\mathbf{P}_{2i+1}^* \end{bmatrix} \mathbf{\Gamma}_p + \mathbb{F}_d^H \begin{bmatrix} \mathbf{S}_{2i} \\ -\mathbf{S}_{2i+1}^* \end{bmatrix} \mathbf{\Gamma}_d \right) \mathbf{h}_{i,sr} + \boldsymbol{\eta}_{i,sr} \quad (7)$$

where:

$$\begin{cases} \mathbb{F}_p^H = \mathbf{I}_2 \otimes \left(\mathbf{F}_N^H \mathbf{Q}_{2N}^{\beta}\right) \\ \mathbb{F}_d^H = \mathbf{I}_2 \otimes \left(\mathbf{F}_N^H \mathbf{Q}_{2N}^{\alpha}\right) \\ \mathbf{\Gamma}_p = [f_{\beta_1}^L, \ldots, f_{\beta_{N_p}}^L]^H \\ \mathbf{\Gamma}_d = [f_{\alpha_1}^L, \ldots, f_{\alpha_{N_d}}^L]^H \\ \mathbf{f}_n^L = [1, e^{j2\pi n/N}, \ldots, e^{j2\pi n(L-1)/N}]^T \end{cases}$$

$$\mathbb{D}_N(\omega_0) = e^{j\omega_0(2iN_q+N_{cp})} \begin{bmatrix} \mathbf{D}_N^{(0)}(\omega_0) & \mathbf{0}_{N\text{x}N} \\ \mathbf{0}_{N\text{x}N} & \mathbf{D}_N^{(1)}(\omega_0) \end{bmatrix} \quad (8)$$

where

$$\mathbf{D}_N^{(u)}(\omega_0) = \text{diag}\left(e^{j(uN_q)\omega_0}, \ldots, e^{j(uN_q+N-1)\omega_0}\right) .$$

$\omega_0 = \Delta\omega_0 T$ is the normalized CFO, $\Delta\omega_0$ is the CFO, and T is the sampling interval and $N_q = N + N_{cp}$.

$$\mathbf{h}_{i,sd}^{(n_r)} = \left[h_{i,sd}^{(n_r)}(0), \ldots, h_{i,sd}^{(n_r)}(L-1)\right]^T$$

and

$$\mathbf{h}_{i,sr} = \left[h_{i,sr}(0), \ldots, h_{i,sr}(L_{sr}-1)\right]^T$$

represent respectively L and L_{sr} taps of channels between source S and the n_r-th receive antenna of the destination node, and the channel between source S and the unique receive antenna at the relay node R.

Vectors $\mathbb{y}_{i,sd}^{(n_r)}$, $\boldsymbol{\eta}_{i,sd}^{(n_r)}$, $\mathbb{y}_{i,sr}$, and $\boldsymbol{\eta}_{i,sr}$ are the received signal and the noise at the n_r-th receive antenna at the destination node D and the received signal and the noise at the relay node R, respectively.

$$\boldsymbol{\eta}_{i,sd}^{(n_r)} = \left[\eta_{i,sd}^{(n_r)}(0), \ldots, \eta_{i,sd}^{(n_r)}(N-1)\right]^T ,$$

and

$$\boldsymbol{\eta}_{i,sr}^{(n_r)} = \left[\eta_{i,sr}(0), \ldots, \eta_{i,sr}(N-1)\right]^T ,$$

are complex additive white Gaussian noise (AWGN) vectors with zero mean and variances $\sigma_{sd}^2\mathbf{I}_N$ and $\sigma_{sr}^2\mathbf{I}_N$, respectively. In the relaying phase, R uses the factor

$$\mathcal{A}_f = \sqrt{p_s \left(p_s \left\|\hat{\mathbf{h}}_{i,sr}\right\|^2 + N_0\right)^{-1}}$$

to adjust the power of the signal received from S, where $\hat{\mathbf{h}}_{sr}$ is the estimated source-relay channel. Then, the second sub-block $[\mathbf{x}_{2i+1}, \mathbf{x}_{2i}^*]$ is generated from the processed versions of received signals at the relay in earlier time slots by adequately applying the conjugation and sign-reversion.

The resulting signals $-\mathcal{A}_f\left[\mathbf{y}_{i,sr}[2]\right]^*$ and $\mathcal{A}_f\left[\mathbf{y}_{i,sr}[1]\right]^*$ are then transmitted to destination node D in time slots 3 and 4, respectively with a power p_r as follows:

$$\begin{aligned}\mathbb{y}_{i,rd}^{(n_r)} &= \begin{bmatrix}\mathbf{y}_{i,rd}^{n_r}[3]\\ \mathbf{y}_{i,rd}^{n_r}[4]\end{bmatrix} = \mathcal{A}_f\sqrt{p_s p_r}\,\mathbb{D}_N(\omega_0)\\ &\cdot\left(\mathbb{F}_p^H\begin{bmatrix}\mathbf{P}_{2i+1}\\ \mathbf{P}_{2i}^*\end{bmatrix}\bar{\mathbf{\Gamma}}_p + \mathbb{F}_d^H\begin{bmatrix}\mathbf{S}_{2i+1}\\ \mathbf{S}_{2i}^*\end{bmatrix}\bar{\mathbf{\Gamma}}_d\right)\mathbf{h}_{i,srd}^{(n_r)} + \mathbb{n}_{i,sd}^{(n_r)}\end{aligned} \tag{9}$$

where

$$\mathbb{n}_{i,srd}^{(n_r)} = \left[(\boldsymbol{\eta}_{2i,srd}^{(n_r)})^T, (\boldsymbol{\eta}_{2i+1,srd}^{(n_r)})^T\right]^T$$

are complex AWGN with $\mathcal{CN}\left(0, (\mathcal{A}_f^2 p_r\sigma_{sr}^2 + \sigma_{rd}^2)\mathbf{I}_N\right)$.

We define the equivalent channel impulse response (CIR) of source-relay-destination ($S-R-D$) links by [12]:

$$\mathbf{h}_{i,srd}^{(n_r)} = \mathrm{conv}(\mathbf{h}_{i,sr}^*, \mathbf{h}_{i,rd}^{(n_r)})\,, \tag{10}$$

where conv means the convolution operation, and $\mathbf{h}_{i,srd}^{(n_r)}$ is $(L_{srd}\times 1)$ vector with $L_{srd} = 2\max(L_{sr}, L_{rd}) - 1$.

$$\bar{\mathbf{\Gamma}}_d = \begin{bmatrix}\bar{\mathbf{f}}_{\alpha_1}^{L_{srd}} & \bar{\mathbf{f}}_{\alpha_2}^{L_{srd}} & \cdots & \bar{\mathbf{f}}_{\alpha_{N_d}}^{L_{srd}}\end{bmatrix}^{\mathcal{H}},$$

$$\bar{\mathbf{\Gamma}}_p = \begin{bmatrix}\bar{\mathbf{f}}_{\beta_1}^{L_{srd}} & \bar{\mathbf{f}}_{\beta_2}^{L_{srd}} & \cdots & \bar{\mathbf{f}}_{\beta_{N_p}}^{L_{srd}}\end{bmatrix}^{\mathcal{H}},$$

are the FFT matrix applied to $\mathbf{h}_{i,srd}^{(n_r)}$, and

$$\begin{aligned}\bar{\mathbf{f}}_n^{L_{srd}} = \big[&e^{j2\pi n(N-\max(L_{sr},L_{rd})+1)/N}, \cdots,\\ &1, \cdots, e^{j2\pi n(\max(L_{sr},L_{rd})-1)/N}\big]^T.\end{aligned}$$

After receiving the signals released from the source and relay nodes at the destination node, we add the signals received at time slots 1 and 3, while applying conjugation before adding the signals received at time slots 2 and 4. The artificially produced signal can be expressed in matrix form as:

$$\begin{aligned}\mathbf{y}_{i,\mathcal{D}}^{(n_r)} &= \begin{bmatrix}\mathbf{y}_{2i,\mathcal{D}}^{(n_r)}\\ \mathbf{y}_{2i+1,\mathcal{D}}^{(n_r)}\end{bmatrix} =\\ \mathbb{D}_N(\omega_0)&\left(\mathbb{F}_p^{\mathcal{H}}\mathbb{P}_i\mathbb{J}_p + \mathbb{F}_d^{\mathcal{H}}\mathbb{S}_i\mathbb{J}_d\right)\begin{bmatrix}\sqrt{p_s}\,\mathbf{h}_{i,sd}^{(n_r)}\\ \mathcal{A}_f\sqrt{p_s p_r}\,\mathbf{h}_{i,srd}^{(n_r)}\end{bmatrix} + \begin{bmatrix}\boldsymbol{\eta}_{2i,\mathcal{D}}^{(n_r)}\\ \boldsymbol{\eta}_{2i+1,\mathcal{D}}^{(n_r)}\end{bmatrix}\end{aligned} \tag{11}$$

$$\begin{cases}\mathbb{J}_p = \begin{bmatrix}\mathbf{\Gamma}_p & \mathbf{0}_{N_p\times L_{srd}}\\ \mathbf{0}_{N_p\times L} & \bar{\mathbf{\Gamma}}_p\end{bmatrix}\\ \mathbb{J}_d = \begin{bmatrix}\mathbf{\Gamma}_d & \mathbf{0}_{N_d\times L_{srd}}\\ \mathbf{0}_{N_d\times L} & \bar{\mathbf{\Gamma}}_d\end{bmatrix}\end{cases} \tag{12}$$

$$\boldsymbol{\eta}_{2i,D}^{(n_r)} = \boldsymbol{\eta}_{2i,sd}^{(n_r)} + \boldsymbol{\eta}_{2i,rd}^{(n_r)}$$

and

$$\boldsymbol{\eta}_{2i+1,D}^{(n_r)} = \boldsymbol{\eta}_{2i+1,sd}^{(n_r)} + \boldsymbol{\eta}_{2i+1,rd}^{(n_r)}$$

are complex AWGN vectors with zero-mean and variance $\sigma_D^2\mathbf{I}_N$ with $\sigma_D^2 = \sigma_{sd}^2 + \mathcal{A}_f^2 p_r\sigma_{sr}^2$.

3. CFO and Channel Estimation

Precise channel and carrier frequency offset (CFO) estimation is essential for reliable data recovery in cooperative DSTBC-OFDM systems, particularly under time-varying channel conditions. The receiver must obtain precise CSI to correctly decode the transmitted signal and apply CFO compensation to mitigate frequency shifts caused by oscillator mismatches or Doppler effects.

A variety of channel estimation methods have been reported for STBC-OFDM systems, broadly categorized into pilot-based and blind approaches. Pilot-based methods embed known training sequences into the transmitted frame, enabling straightforward channel estimation at the receiver. On the contrary, blind methods exploit the statistical properties of the received signal to infer the channel without explicit training [14]. Although blind estimation reduces overhead, it generally requires longer observation intervals and is less robust under severe fading or time-varying conditions.

For cooperative systems, joint estimation of CFO and CSI has been explored in prior works. For example, papers [15]-[19] present a semi-blind joint estimation method for MIMO STBC-OFDM systems. However, such schemes often assume multiple antennas at each node, which may be impractical in many wireless devices due to size and cost constraints. Moreover, propagation conditions may not consistently support full MIMO specifications in real deployments.

In Tab. 2 summary of selected literature on channel and CFO estimation in STBC-OFDM systems is provided.

In the simulation framework of this study, pilot-assisted CSI estimation and a CFO estimation scheme that combines pilot symbols and virtual subcarriers (VSCs) are implemented for AF-based cooperative DSTBC-OFDM. The AF protocol is adopted for its low implementation complexity, despite its inherent noise amplification effect, as it remains competitive in performance compared to decode and forward (DF) under the considered channel conditions.

This estimation approach provides the necessary preprocessing for the subsequent benchmarking of modulation classifiers. By standardizing the CFO and CSI estimation across all classifiers, the evaluation isolates the classification performance from the variability related to the estimation, ensuring a fair and consistent comparison.

By assuming $\hat{\omega}_0 = \omega_0$ in Eq. (8), we can recover $\hat{\mathfrak{h}}^{(n_r)}$ by solving a least-square (LS) problem, as:

$$\hat{\mathfrak{h}}_i^{(n_r)} = e^{-j\hat{\omega}_0(2iN_q+N_{cp})}\left(\mathbb{P}_i\mathbb{J}_p\right)\mathbb{F}_p\mathbb{D}_N^{\mathcal{H}}(\hat{\omega}_0)\mathbb{y}_{i,\mathcal{D}}^{(n_r)}\,. \tag{13}$$

Based on VSCs, the blind CFO estimate is obtained by minimizing the following quadratic cost function:

$$\mathcal{J}^{(n_r)}(\hat{\omega}_0) = \frac{1}{N_b}\sum_{i=0}^{N_b-1}\left\|e^{-j(2iN_q+N_{cp})\hat{\omega}_0}\mathbb{F}_z\mathbb{D}_N^H(\hat{\omega}_0)\mathbb{y}_{i,D}^{(n_r)}\right\|^2 \tag{14}$$

where

$$\begin{cases} \mathbb{F}_z = \begin{bmatrix} \mathbf{F}_z & \mathbf{0}_{N_{vsc}\times N} \\ \mathbf{0}_{N_{vsc}\times N} & \mathbf{F}_z \end{bmatrix} \\ \mathbf{F}_z^{\mathcal{H}} = \begin{bmatrix} \mathbf{f}_{N_e+1}^{\mathcal{N}} & \cdots & \mathbf{f}_N^{\mathcal{N}} \end{bmatrix} \end{cases} . \tag{15}$$

We compensate the received signal by the estimated CFO; then, we perform demodulation using $\mathbb{F}_d$. Next, we use estimated channels to recover the transmitted data employing the zero-forcing equalizer:

$$\mathbb{H}_i^{(n_r)} = \begin{bmatrix} \tilde{\mathrm{H}}_{i,sd}^{(n_r)} & \tilde{\mathrm{H}}_{i,srd}^{(n_r)} \\ \left(\tilde{\mathrm{H}}_{i,srd}^{(n_r)}\right)^* & -\left(\tilde{\mathrm{H}}_{i,sd}^{(n_r)}\right)^* \end{bmatrix} , \tag{16}$$

where

$$\tilde{\mathrm{H}}_{i,sd}^{(n_r)} = \sqrt{p_s}\mathrm{D}_N\left(\tilde{h}_{i,sd}^{(n_r)}\right)$$

and

$$\tilde{\mathrm{H}}_{i,srd}^{(n_r)} = \mathcal{A}_f\sqrt{p_s p_r}\mathrm{D}_N\left(\tilde{h}_{i,srd}^{(n_r)}\right)$$

are the frequency-response of the equivalent channel between the source node and the n_r-th receive antenna, in the direct and indirect link, respectively.

The recovered data symbols are given by:

$$\begin{cases} \hat{\mathbf{s}}_{2i} \\ \hat{\mathbf{s}}_{2i+1} \end{cases} = e^{-j\hat{\omega}_0(2iN_q+N_{cp})} \sum_{n_r=1}^{N_r} \left(\mathbf{H}_i^{(n_r)}\right)^H \begin{bmatrix} \mathbf{F}_d & \mathbf{0} \\ \mathbf{0} & \mathbf{F}_d^* \end{bmatrix} \cdot \begin{bmatrix} \mathbf{D}_N^{(0)}(\hat{\omega}_0) & \mathbf{0}_{N\times N} \\ \mathbf{0}_{N\times N} & \mathbf{D}_N^{(1)}(\hat{\omega}_0) \end{bmatrix} \begin{bmatrix} \mathbf{y}_{D,2i}^{(n_r)} \\ -\left(\mathbf{y}_{D,2i+1}^{(n_r)}\right)^* \end{bmatrix} . \tag{17}$$

4. Modulation Classification Algorithms

A standard digital modulation classification (DMC) system consists of two main subsystems: feature extraction and classification. The feature extraction subsystem typically includes a pre-processing stage followed by feature selection.

Effective pre-processing – such as CFO compensation and channel equalization – plays a crucial role in improving modulation identification performance. Proper pre-processing facilitates more reliable feature extraction, thus improving classifier accuracy. In contrast, inadequate pre-processing can significantly degrade classification results [14].

Previous studies [9], [13], [14] have demonstrated that higher-order cumulants (HOC) and higher-order moments (HOM) serve as effective features for modulation classification, offering a favorable trade-off between classification performance and computational complexity. In this work, we extract the features comprising HOM up to the eighth order and HOC up to the sixth order to form higher order T statistics (HOS) vectors [28]. These feature vectors are subsequently processed using principal component analysis (PCA) before being input into the classifiers.

The feasibility of deploying a model on real hardware depends largely on selecting trainable parameters from candidate features, as these directly impact computational cost. To address this, PCA is used to compress the original dataset vector D_g into a lower-dimensional dataset D_s, effectively removing redundant and irrelevant information. This reduction in dimensionality enables the selection of an optimal subset of HOS that improves the precision of modulation identification while minimizing computational complexity [29].

The optimized feature subset is then fed into the classifiers to accurately differentiate between various linear modulation schemes.

4.1. Classification Tools

Digital modulation classification (DMC) plays a crucial role in the definition of an intelligent receiver. Numerous studies have explored modulation recognition using either single or ensemble learning algorithms. A single learning algorithm employs one classifier model, whereas ensemble learning combines multiple weaker classifiers to form a more robust predictor.

In this work, we use feedforward neural networks (FFNN) and support vector machines (SVM) as single-learning algorithms. For ensemble learning, we employ random forest classifier (RFC) and AdaBoost, representing bagging and booster methods, respectively.

FFNNs are a popular choice for trainable pattern classification due to their straightforward architecture, where information flows sequentially from one layer to the next [15]. The network consists of three types of layers: input, hidden, and output. The input layer receives external data to initiate pattern recognition. The hidden layers process this information through weighted connections, and the output layer produces the classification result [30].

In this study, FFNN training begins by feeding the selected feature subset a_i into the input layer to predict the corresponding label N_i. After training, performance is evaluated during the testing phase by measuring the probability of correct identification. The final decision is made by selecting modulation type from the candidate pool Θ ={2PSK, 8PSK, 8PAM, 16QAM}, and presented by the label vector θ_i of length equal to cardinal of Θ.

Selection of Θ provides a comprehensive baseline for evaluating the performance of the communication system in different modulation domains. 2PSK, with its simple two-point phase constellation, offers robustness against noise and serves as a clear reference for low-complexity scenarios. 8PSK increases spectral efficiency by encoding three bits per symbol through phase variations, allowing the evaluation of system behavior under moderate complexity. 8PAM, varying only in amplitude, provides insight into amplitude-sensitive impairments and complements phase-based evaluations. Finally, 16QAM combines amplitude and phase to encode four bits per symbol and represents a standard high-throughput modulation widely used in modern systems, making it a realistic baseline for practical applications.

Collectively, these schemes cover phase-only, amplitude-only, and combined amplitude-phase modulations, providing

Tab. 2. Summary of selected literature on channel and CFO estimation in STBC-OFDM systems. The symbol "×" indicates that the survey did not review a classification method.

Ref.	Classification method	System	Contribution
[7]	×	Cooperative STBC OFDM	Analyzes the impact of CFO and channel estimation errors on LS receiver performance; derives closed-form expressions for output SNR evaluation
[20]	×	MIMO OFDM	Proposes a PARAFAC-based blind channel estimation method using recursive least squares tracking, improving estimation accuracy by minimizing uncertainty via weighted least squares cost function
[21]	×	MIMO OFDM	Proposes iterative joint ML CFO and channel estimators for asynchronous cooperative systems, reducing complexity via SAGE-based iterative estimation (SAGE-IE)
[22]	Maximum likelihood-based multi-cumulant classification	MIMO	Proposes a feature-based AMC framework using blind channel estimation and multi-cumulant vectors combining arbitrary orders and lags. Introduces natural ICA and fast ICA methods to improve channel estimation and classification accuracy
[23]	Support vector machines	SISO	Examines the impact of phase offset estimators, channel state information, and noise on classification accuracy
[24]	DNN and ML-based classifiers	SISO	Studies modulation classification by mapping signal samples to posterior probabilities; demonstrates robustness under uncertain channels and noise
[25]	×	SISO OFDM	Proposes a blind CFO estimation method using DCT/IDCT frequency-domain symmetry combined with equalization via banded-matrix approximation to improve system performance
[26]	×	STBC MIMO OFDM	Proposes a Kalman-filter-based channel estimation method combined with STBC and orthogonal pilot sequences to enhance diversity gains and mitigate antenna interference
[27]	×	SISO OFDM	Models joint estimation of CFO, sparse channel, and noise statistics, addressing challenges of sparse signal recovery with unknown CFO and noise variance

a scalable framework for baseline evaluation while enabling future extension to more complex constellations, such as higher-order QAM or adaptive hybrid schemes.

Similarly to the FFNN, SVM can be a global approximator of any multivariate function for an undefined level of accuracy. It is used in DMC due to the efficiency and capacity of treating high-dimensional data with a few needed parameters.

When the pattern recognition assignments are manageable, SVM uses hyperplanes to separate data linearly and with maximal boundaries. When a given class cannot be linearly separated in the input space, SVM converts this input space into a high-dimensional feature space.

Tab. 3. Theoretical values of selected HOM and HOC for various modulation types [30].

Type	M_{60}	M_{61}	M_{63}	C_{60}	C_{61}	C_{63}
2PSK	1	1	1	16	16	16
8PSK	0	0	1	0	0	4
8PAM	3.62	3.62	3.62	7.19	7.19	7.19
16QAM	0	0.38	2.08	0	1.8	1.8

We use the "one-against-all" (OAA) method for the multi-class classification of SVM. Furthermore, we engage cross-validation, a standard form of validation technique usually adopted in the training stage to serve as a performance metric to avoid overfitting [31].

The random forest classifier (RFC) is constructed from a set of learners, and it uses decision trees as the base learners. Each learner votes on the class labels to make a final prediction.

The property of being an aggregation of multiple learners enables RFC to be prominent over conventional classification trees [17]. AdaBoost is designed to transform weak learners – in this paper, decision trees – into strong ones, to reach the highest accuracy level [18]. Different learners are trained sequentially by including a new learner per cycle to compensate for inaccuracies created by former learners.

When the cycle ends, the low weight samples acquired are the ones that the weak learner H_t had accurately classified, but the misclassified examples are identified and emphasized

to be fed back into the beginning of the subsequent round, then the new learner H_t is trained.

The previous procedure extends for several rounds. Eventually, AdaBoost forms an ultimate hypothesis using weighted votes to combine all the weak learners [19].

5. Simulation Results

A set of experiments was carried out to assess the performance of the proposed method employing Monte Carlo simulations. We evaluate the performance of CFO and channel estimators by calculating the bit error rate (BER) of CFO, the mean square errors (MSE) of CFO and channels. The MSEs of CFO and channel estimators are defined respectively by:

$$\mathrm{MSE}_{\mathrm{CFO}} = \frac{1}{M_c}\sum_{j=1}^{M_c}\left|\hat{\omega}_0^j - \omega_0\right|^2, \tag{18}$$

$$\mathrm{MSE}_{\mathrm{Channel}} = \frac{1}{M_c N_r}\sum_{j=1}^{M_c}\sum_{n_r=1}^{N_r}\left\|\hat{\mathbf{h}}_j^{(n_r)} - \mathbf{h}^{(n_r)}\right\|^2. \tag{19}$$

The proposed approach was validated for the digital modulation pool Θ=2PSK, 8PSK, 8PAM, 16QAM. 1000 Monte Carlo trials per modulation were carried out for each SNR value.

We consider the SNR across source-relay link SNR_{sr} and the SNR across relay–destination links SNR_{rd} is $\mathrm{SNR} = \mathrm{SNR}_{rd} = \mathrm{SNR}_{sr}$.

We generated a random massage and $L = L_{sr} = L_{rd}$ Rayleigh fading taps channel from i.i.d. zero-mean independent complex Gaussian random variables with the same variance in each run.

We calculate the average classification accuracy for different values of SNR to analyze the performance of the proposed classifier.

Simulations are performed considering an OFDM system with $N = 64$ and 512 subcarriers, and with a cyclic prefix of length $N_{cp} = L + 1$. We consider a single relay for all the experiments and the STBC encoder type Alamouti with (2×1) $(N_r = 1)$ and (2×2) $(N_r = 2)$ antenna configurations are inspected.

Regarding the MUSIC-based CFO estimator for the cooperative DSTBC-OFDM system, we note that it has a complexity order of $O(12N^2N_bN_rG)$, where G is the number of CFO candidates, $\hat{\omega}_0$ in the search grid.

We employ the parameters specified in Tab. 4 to confirm the highest integrity and consistency of the classifier comparison.

5.1. Performance of CFO and Channels Estimation

A set of experiments was conducted to compare the performance between the estimated CFO and channels and the exact CFO and channels for the cooperative DSTBC-OFDM system. Figure 2 shows the BER versus SNR. Pool Θ contains the modulation types for the comparison. The source and relay nodes are occupied by one antenna at each, while $N_r = 2$ receive antennas occupy the destination node.

Tab. 4. Simulation parameters.

Parameter	Value
Dataset	D_g
Modulation pool	4 digital modulations: Θ={2PSK, 8PSK, 8PAM, 16QAM}
Number of data subcarriers	$\begin{cases} N_d = 51 \text{ for } N = 64 \\ N_d = 443 \text{ for } N = 512 \end{cases}$
Number of pilots subcarriers	$\begin{cases} N_p = 8 \text{ for } N = 64 \\ N_p = 64 \text{ for } N = 512) \end{cases}$
Number of virtual subcarriers	$N_{vsc} = 5$
Signal format	In-phase and quadrature (IQ)
Signal dimension	$2 \times 64/2 \times 512$ per time-slot
SNR range	$[-5, 0, \ldots, 15, 20]$ dB
CFO range	[0, 0.1]
CFO candidate	$0.02\,\pi$
Monte Carlo trials	$M_c = 1000$ for each modulation type

The performance of the system using the proposed estimated CFO and channel parameters closely matches that achieved with exact CFO and perfect channel knowledge, demonstrating the reliability of the estimators. For modulation schemes such as 2PSK, 8PSK, 8PAM, and 16QAM, the performance difference between the proposed estimation method and the ideal case is negligible. However, for 16QAM, a relatively larger performance gap is observed, likely due to the increased constellation size, which typically leads to greater system degradation.

5.2. MSE of CFO and Channels Estimators

To evaluate the reliability of the proposed CFO and channel estimation methods, Figs. 3a and 3b present the MSE of the CFO and channel estimates plotted against the SNR, respectively.

The results indicate that changing the modulation scheme does not significantly impact the CFO MSE. In contrast, the accuracy of the CFO estimation is consistent, as the SNR increases for all types of modulation types within the set Θ.

Figure 3b confirms that the proposed channel estimator performs better with increasing SNR.

5.3. Robustness Tests

This subsection evaluates the robustness of the proposed estimation technique by examining the classification performance of various classifiers combined with principal component analysis (PCA).

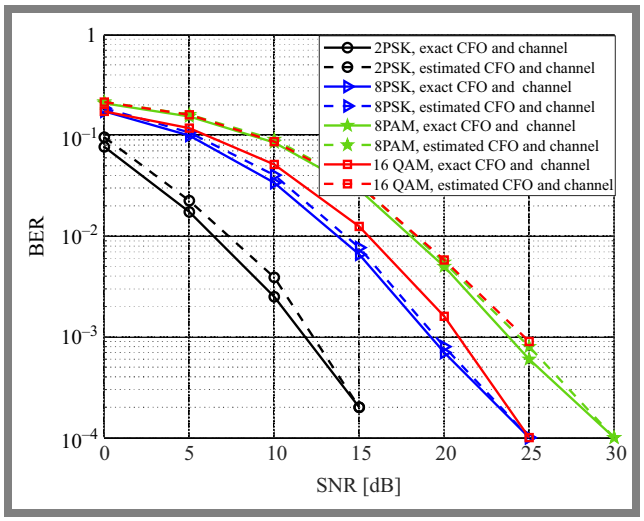

Fig. 2. BER versus SNR of the cooperative DSTBC-OFDM system in the presence of CFO and channel estimation for $N_r = 2$ and $N = 512$.

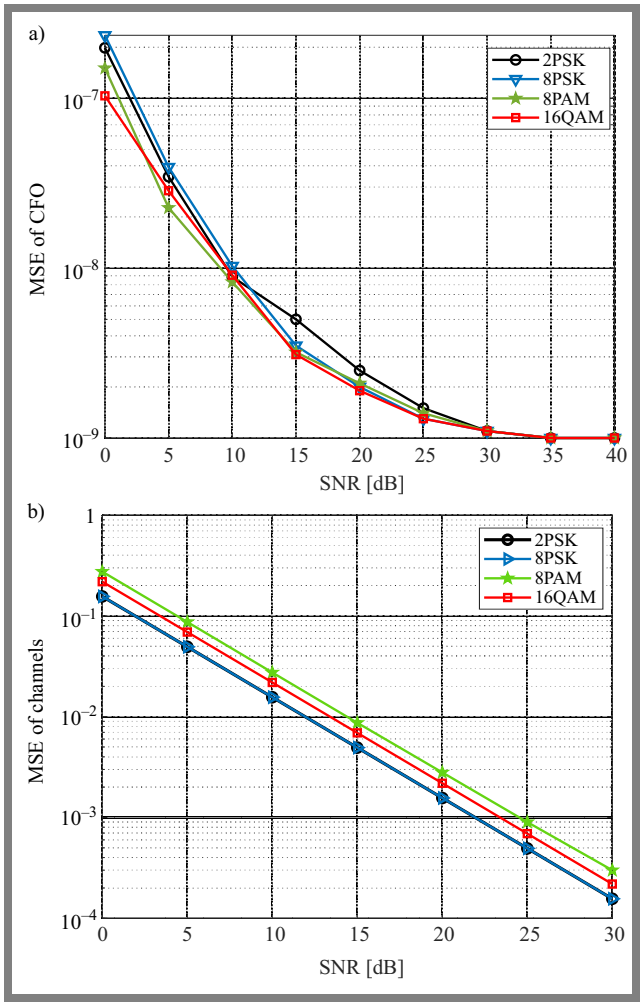

Fig. 3. MSE of the CFO estimator a) MSE of channel estimator b) versus SNR of cooperative DSTBC-OFDM system for $N = 512$ and $N_r = 2$.

The study investigates the impact of the size of the OFDM symbol N and the number of receiving antennas N_r on classification accuracy. The parameters used are summarized in Tab. 4. Specifically, OFDM symbol sizes of N= 64 and 512 are considered, alongside two antenna configurations: 2×1 and 2×2.

Figure 4a presents the average classification accuracy of different classifiers using estimated CFO and channel parameters, with the number of receiving antennas fixed at N_r= 2. An increase in classification accuracy is observed as N increases from 64 to 512, attributed to improved time diversity of the received signals that benefits all classifiers. At N= 64, all classifiers perform similarly, achieving an average accuracy of 92% at SNR = 10 dB. For SNR 15 dB, accuracy rises to approximately 98%.

When N= 512, FFNN and RFC outperform other classifiers, reaching 66% classification accuracy at SNR = 0 dB. SVM and AdaBoost follow closely, with average accuracies of 60% and 58%, respectively. At SNR = 5 dB, all classifiers have 94% accuracy, and achieve 100% accuracy for SNR $\geqslant$ 10 dB.

Figure 4b illustrates the probability of correct identification versus SNR considering 2×1 and 2×2 antenna configurations with N=512. All classifiers show stable performance, with classification accuracy improving as N_r increases from 1 to 2. For example, at SNR = 5 dB and N_r=2, all classifiers reach 94% accuracy. In contrast, at the same SNR with N_r= 1, RFC and SVM achieve 62% accuracy, while AdaBoost and FFNN outperform them with 84% and 78% accuracy, respectively. For N_r= 2 and SNR $\geqslant$ 10 dB, all classifiers achieve 100% accuracy.

At N_r= 1 and SNR = 10 dB, AdaBoost and FFNN perform similarly, achieving 100% accuracy, whereas SVM and RFC attain 90% and 88%, respectively. For SNR $\geqslant$ 15 dB, all classifiers reach 98% accuracy.

Such results confirm that high classification accuracy can be achieved even at low SNR levels. These results reflect the effectiveness of the proposed CFO and channel estimation techniques. Among the classifiers tested, FFNN and AdaBoost consistently deliver superior performance at SNR $\geqslant$ 10 dB, reaching 100% accuracy regardless of antenna configuration and OFDM symbol length.

5.4. Performance Comparison and Evaluation

Figure 5 compares the average classification precision achieved using the proposed CFO and channel estimation method against the ideal case with exact CFO and perfect channel knowledge. The comparison is performed for classifiers under the parameters listed in Tab. 4, with an OFDM symbol size $N = 512$ and the number of receive antennas $N_r = 2$.

The results demonstrate that the proposed estimation method achieves a classification accuracy that closely matches the ideal case at SNR = 5 dB and attains near-perfect accuracy for SNR values greater than 5 dB. This confirms the robustness across all classifiers under low SNR conditions.

At SNR = 5 dB, the benchmarking shows that among FFNN, RFC, SVM, and AdaBoost, FFNN provides the highest accuracy and robustness. At SNR = 0 dB, FFNN and RFC

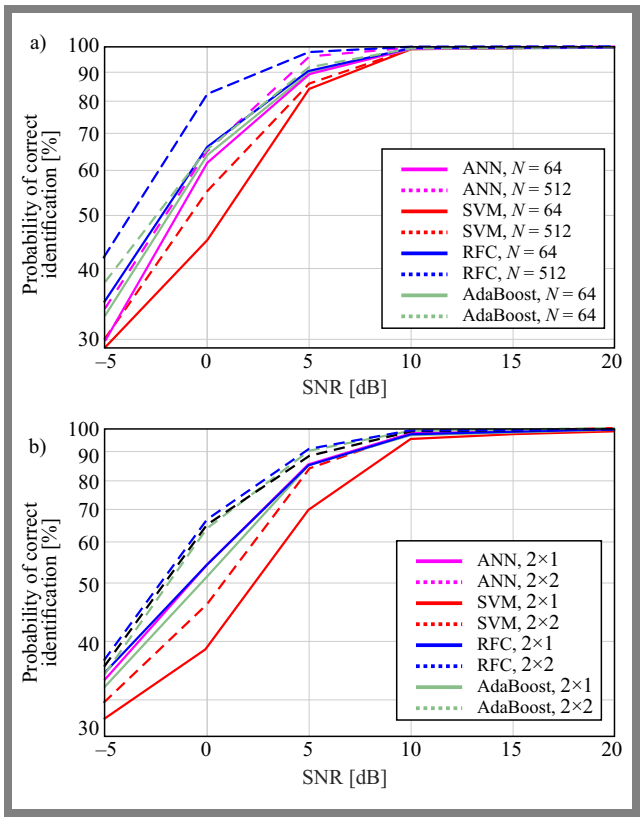

Fig. 4. Classification performance vs. SNR with estimated CFO and channels for: $N_r = 2$, OFDM symbol length $N = 512, 64$ a) and $N_r = 1, 2$, $N = 512$ b).

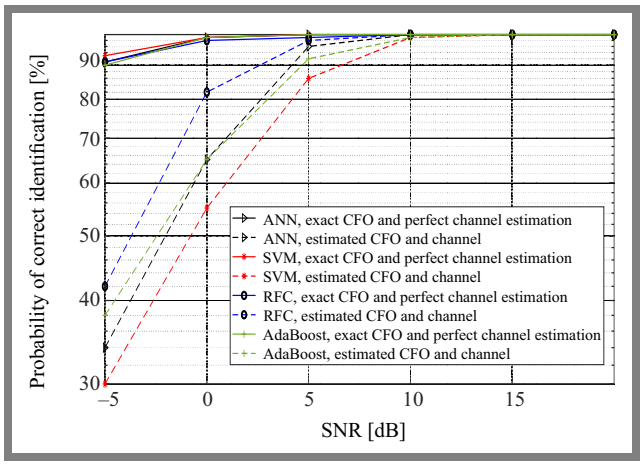

Fig. 5. Classification performance vs. SNR system with estimated CFO and channel and with exact CFO and perfect channel estimated for $N = 512$ and $N_r = 2$.

outperform the other classifiers in distinguishing between different linear modulation schemes.

In general, this benchmarking study reveals that the proposed CFO and channel estimation technique significantly improves the performance of the system in cooperative DSTBC-OFDM environments, reaching near-ideal classification accuracy at SNR 5 dB. Furthermore, FFNN consistently provides superior classification performance in low SNR regimes (below 0 dB), highlighting its suitability for poor channel conditions.

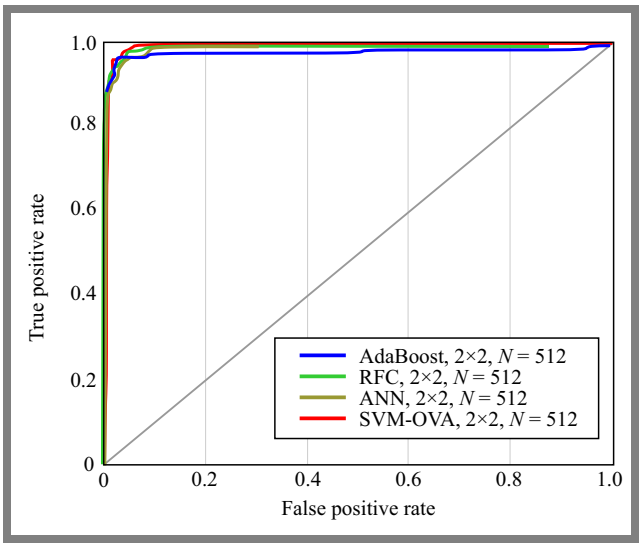

Fig. 6. ROC curves of the ANN, SVM, RFC and AdaBoost classifiers using DSTBC-OFDM with exact CFO and perfect channel estimated for $N = 512$ and $N_r = 2$.

In Fig. 6, the receiver operating characteristic (ROC) curves for AdaBoost, RFC, ANN, and support vector machine using one-versus-all (SVM-OVA) are presented for the 2×2 classification scenario with N= 512 samples. ROC curves are generated using the average posterior probabilities computed in all SNR values ranging from –5 to 20 dB, thereby reflecting the aggregated detection performance under varying noise conditions.

All four classifiers demonstrate strong discriminative capability, as their ROC curves remain close to the upper left region of the plot. AdaBoost, RFC, and ANN exhibit nearly overlapping curves, indicating comparable and consistently high classification performance over the full SNR range. The SVM-OVA classifier achieves a similar overall trend, although minor deviations appear in mid-range false-positive regions.

The close proximity of the curves to the ideal operating point (0,1) suggests that averaging over SNR does not significantly degrade model performance, and all classifiers maintain high true-positive rates with minimal false-positive rates across noise levels. These results confirm that the ensemble-based methods and the neural network provide robust performance under varying SNR conditions, while SVM-OVA remains competitive with slightly higher variability.

6. Conclusions

This paper presented a comprehensive benchmarking study of blind modulation classification in cooperative DSTBC-OFDM systems under realistic impairments, including carrier frequency offset (CFO) and imperfect channel state information (CSI). A hybrid estimation approach combining pilot symbols and virtual subcarriers (VSCs) for CFO estimation with pilot-assisted CSI estimation was developed, leading to improved synchronization accuracy and system reliability.

Using higher-order statistics (HOS) as features, several machine learning classifiers – feedforward neural networks (FFNN), support vector machines (SVM), random forest classifier (RFC) and adaptive boosting (AdaBoost) – were evaluated under varying SNR and fading conditions. Results show that while the proposed estimation scheme effectively mitigates CFO and channel distortions, classifier performance differs across scenarios, with FFNN and AdaBoost achieving the highest accuracy, particularly under low SNR conditions.

References

[1] H. Tayakout, I. Dayoub, K. Ghanem, and H. Bousbia-Salah, "Automatic Modulation Classification for D-STBC Cooperative Relaying Networks", *IEEE Wireless Communications Letters*, vol. 7, pp. 780–783, 2018 (https://doi.org/10.1109/LWC.2018.2824813).

[2] G. Ryu, D. Jang, U. Jeong, and K. Ko, "BER Performance Analysis of Orthogonal Space-time Block Codes in Cooperative MIMO DF Relaying Networks", *IEEE International Conference on Communications (ICC)*, Kansas City, USA, 2018 (https://doi.org/10.1109/ICC.2018.8423038).

[3] W. Swasdio, C. Pirak, S. Jitapunkul, and G. Ascheid, "Alamouti-coded Decode-and-forward Protocol with Optimum Relay Selection and Power Allocation for Cooperative Communications", *Journal of Wireless Communications and Networking*, vol. 2014, art. no. 112, 2014 (https://doi.org/10.1186/1687-1499-2014-112).

[4] A. Abdaoui, S.S. Ikki, and M.H. Ahmed, "Performance Analysis of MIMO Cooperative Relaying System Based on Alamouti STBC and Amplify-and-forward Schemes", *IEEE International Conference on Communications (ICC)*, Cape Town, South Africa, 2010 (https://doi.org/10.1109/ICC.2010.5501917).

[5] S. Yiu, D. Calin, O. Kaya, and K. Yang, "Distributed STBC-OFDM and Distributed SFBC-OFDM for Frequency-selective and Time-varying Channels", *IEEE Wireless Communications and Networking Conference (WCNC)*, Paris, France, 2012 (https://doi.org/10.1109/WCNC.2012.6214222).

[6] E. Chenguttuvan, L.P. Karuppiah, and K. Sakthisudhan, "Estimating Time and Frequency Under Imperfect Channel Knowledge Using ECM and SAGE Algorithms in Multi-relay Cooperative Networks", *Journal of Wireless Communications and Networking*, vol. 2025, art. no. 1, 2025 (https://doi.org/10.1186/s13638-024-02418-9).

[7] T. Lin and F. Hwang, "Analysis and Design of Joint CFO/Channel Estimate Techniques for a Cooperative STBC-OFDM System", *International Journal of Communication Systems*, vol. 32, art. no. e3845, 2018 (https://doi.org/10.1002/dac.3845).

[8] M. Besseghier *et al.*, "Enhanced Estimation of Channel and CFO in FBMC/OQAM via ZFBMC-based Preamble", *Wireless Personal Communications*, vol. 139, pp. 1815–1836, 2024 (https://doi.org/10.1007/s11277-024-11701-3).

[9] K. Hassan *et al.*, "Blind Digital Modulation Identification for Spatially Correlated MIMO Systems", *IEEE Transactions on Wireless Communications*, vol. 11, pp. 683–693, 2012 (https://doi.org/10.1109/TWC.2011.122211.110236).

[10] B. Xu *et al.*, "Towards Explainability for AI-based Edge Wireless Signal Automatic Modulation Classification", *Journal of Cloud Computing*, vol. 13, art. no. 10, 2024 (https://doi.org/10.1186/s13677-024-00590-3).

[11] K. Akhilesh and K. Vinay, "A Review of Diverse MIMO Antennas Design for Cognitive Radio Applications", *AEU – International Journal of Electronics and Communications*, vol. 200, art. no. 155930, 2025 (https://doi.org/10.1016/j.aeue.2025.155930).

[12] M. Besseghier, A.B. Djebbar, A. Zouggaret, and I. Dayoub, "Joint Channel Estimation and Data Detection for OFDM Based Cooperative System", *Telecommunication Systems*, vol. 73, pp. 545–556, 2019 (https://doi.org/10.1007/s11235-019-00622-3).

[13] Q. Xiao *et al.*, "Research on OFDM Modulation Recognition Method Based on High-order Cyclic Cumulants and Neural Networks", *IEEE 6th International Conference on Power, Intelligent Computing and Systems (ICPICS)*, Shenyang, China, pp. 712–716, 2024 (https://doi.org/10.1109/ICPICS62053.2024.10796030).

[14] M. Ghogho and A. Swami, "Semi-blind Frequency Offset Synchronization for OFDM", *IEEE International Conference on Acoustics, Speech, and Signal Processing (ICASSP)*, Orlando, USA, 2002 (https://doi.org/10.1109/ICASSP.2002.5745113).

[15] X. Ma, M.K. Oh, G.B. Giannakis, and D.J. Park, "Hopping Pilots for Estimation of Frequency-offset and Multiantenna Channels in MIMO-OFDM", *IEEE Transactions on Communications*, vol. 53, pp. 162–172, 2005 (https://doi.org/10.1109/TCOMM.2004.840663).

[16] R.N. Yang, W.T. Zhang, and S.T. Lou, "Joint Adaptive Blind Channel Estimation and Data Detection for MIMO-OFDM Systems", *Wireless Communications and Mobile Computing*, vol. 2020, art. no. 2508130, 2020 (https://doi.org/10.1155/2020/2508130).

[17] B. Dehri, M. Besseghier, A.B. Djebbar, and I. Dayoub, "Blind Digital Modulation Classification for STBC-OFDM System in Presence of CFO and Channels Estimation Errors", *IET Communications*, vol. 13, pp. 2827–2831, 2019 (https://doi.org/10.1049/iet-com.2019.0362).

[18] T. Liu and S. Zhu, "Joint CFO and Channel Estimation for Asynchronous Cooperative Communication Systems", *IEEE Signal Processing Letters*, vol. 19, pp. 643–646, 2012 (https://doi.org/10.1109/LSP.2012.2210039).

[19] S. Huang *et al.*, "Automatic Modulation Classification of Overlapped Sources Using Multiple Cumulants", *IEEE Transactions on Vehicular Technology*, vol. 66, pp. 6089–6101, 2017 (https://doi.org/10.1109/TVT.2016.2636324).

[20] K. Ramadan, M.I. Dessouky, and F.E. El-Samie, "Joint Equalization and CFO Compensation for Performance Enhancement of MIMO-OFDM Communication Systems Using Different Transforms with Banded-matrix Approximation", *AEU – International Journal of Electronics and Communications*, vol. 119, art. no. 153157, 2020 (https://doi.org/10.1016/j.aeue.2020.153157).

[21] R. Tang, X. Zhou, and C. Wang, "Kalman Filter Channel Estimation in 2x2 and 4x4 STBC MIMO-OFDM Systems", *IEEE Access*, vol. 8, pp. 189089–189105, 2020 (https://doi.org/10.1109/ACCESS.2020.3027377).

[22] S. Salari and F. Chan, "Joint CFO and Channel Estimation in OFDM Systems Using Sparse Bayesian Learning", *IEEE Communications Letters*, vol. 25, pp. 166–170, 2021 (https://doi.org/10.1109/LCOMM.2020.3024817).

[23] J. Jagannath, N. Polosky, and D. O'Connor, "Artificial Neural Network Based Automatic Modulation Classification over a Software Defined Radio Testbed", *IEEE International Conference on Communications (ICC)*, Kansas City, USA, 2018 (https://doi.org/10.1109/ICC.2018.8422346).

[24] S. Huang *et al.*, "Automatic Modulation Classification of Overlapped Sources Using Multiple Cumulants", *IEEE Transactions on Vehicular Technology*, vol. 66, pp. 6089–6101, 2017 (https://doi.org/10.1109/TVT.2016.2636324).

[25] A. Swami and B. Sadler, "Hierarchical Digital Modulation Classification Using Cumulants", *IEEE Transactions on Communications*, vol. 48, pp. 416–429, 2000 (https://doi.org/10.1109/26.837045).

[26] K.A. Ahmed and E. Ergun, "Automatic Modulation Classification Using Different Neural Network and PCA Combinations", *Expert Systems with Applications*, vol. 175, art. no. 114931, 2021 (https://doi.org/10.1016/j.eswa.2021.114931).

[27] I. Klyueva, "Improving Quality of the Multiclass SVM Classification Based on the Feature Engineering", *1st International Conference on Control Systems, Mathematical Modelling, Automation and Energy Efficiency (SUMMA)*, Lipetsk, Russia, pp. 491–494, 2019 (https://doi.org/10.1109/SUMMA48161.2019.8947599).

[28] O.P. Awe, A. Deligiannis, and S. Lambotharа, "Spatio-temporal Spectrum Sensing in Cognitive Radio Networks Using Beamformer-

aided SVM Algorithms", *IEEE Access*, vol. 6, pp. 25377–25388, 2018 (https://doi.org/10.1109/ACCESS.2018.2825603).

[29] K. Triantafyllakis, M. Surligas, and G. Vardakis, "Phasma: An Automatic Modulation Classification System Based on Random Forest", *IEEE International Symposium on Dynamic Spectrum Access Networks (DySPAN)*, Piscataway, USA, 2017 (https://doi.org/10.1109/DySPAN.2017.7920749).

[30] S. Yuan *et al.*, "Efficient and Privacy-preserving Outsourcing of Gradient Boosting Decision Tree Inference", *IEEE Transactions on Services Computing*, vol. 17, pp. 2334–2348, 2024 (https://doi.org/10.1109/TSC.2024.3395928).

[31] Y. Zhou *et al.*, "A Modulation Recognition Method Based on Bispectrum and Ensemble Learning", *2nd International Conference on Computer Science, Electronic Information Engineering and Intelligent Control Technology (CEI)*, Nanjing, China, pp. 124–128, 2022 (https://doi.org/10.1109/CEI57409.2022.9950111).

Brahim Dehri, Ph.D.
Telecommunications and Digital Signal Processing Laboratory
https://orcid.org/0000-0002-9106-6931
E-mail: dehri.brahim@cuniv-naama.dz
University Centre of Naama, Naama, Algeria
https://www.cuniv-naama.dz

Hakima Moulay, Ph.D.
Telecommunications and Digital Signal Processing Laboratory
https://orcid.org/0000-0002-5637-3944
E-mail: moulay.hakima@cuniv-naama.dz
University of Sidi Bel Abbes, Sidi Bel Abbes, Algeria
https://www.univ-sba.dz/en

Ahmed Amine Daikh, Ph.D.
LIS2T Laboratory
https://orcid.org/0000-0002-4666-2750
E-mail: aadaikh@cuniv-naama.dz
University Centre of Naama, Naama, Algeria
https://www.cuniv-naama.dz
University of Mustapha Stambouli, Mascara, Algeria
https://www.univ-mascara.dz

Mokhtar Besseghier, Ph.D.
LIS2T Laboratory
https://orcid.org/0000-0003-3522-1332
E-mail: m.besseghier@univ-mascara.dz
University of Mustapha Stambouli, Mascara, Algeria
https://www.univ-mascara.dz